A Study of Performance Enhancement in Uniaxial Stressed Silicon Nanowire Field Effect Transistors

Hyo-Eun Jung, Woo Jin Jeong, and Mincheol Shin
Dept. of Electrical Engineering, Korea Advanced Institute of Science and Technology, Korea
Email: junghe@kaist.ac.kr, jee-nee0919@kaist.ac.kr, mshin@kaist.ac.kr

***Abstract*—The performance of uniaxially strained Si nanowires (SiNWs) is investigated with the multiband *k.p* method. A rigorous quantum-mechanical calculation of hole current based on the non-equilibrium Green's function (NEGF) method is carried out. For both unstrained/strained-SiNWs, the necessity of using the tuned *k.p* parameters instead of the bulk *k.p* parameters for nano-scaled devices is examined by benchmarking with the tight-binding (TB) method. The on-current characteristics of the unstrained/strained-SiNWs are analyzed as a function of the aspect ratio of channel length (L) and width (W). The amount of on-current increase due to strain is quantitatively calculated, which shows an increasing behavior with respect to L/W.**

Keywords*— *k.p, strain, nanowire, MOSFET, quantum transport, non-equilibrium Green's function

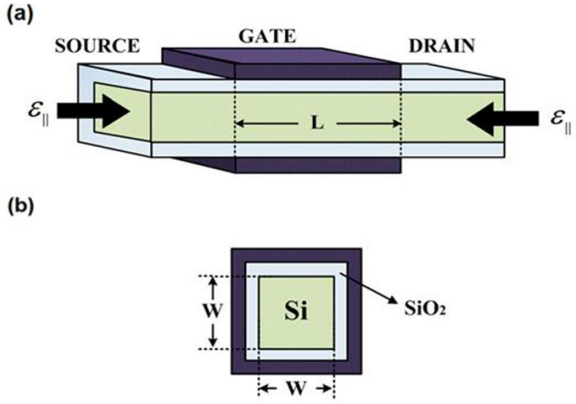

Fig. 1: (a) Schematic diagram of gate-all-around p-type silicon nanowire FETs with the uniaxial compressive strain. (b) Cross-sectional view at the center of the channel.

I. Introduction

Strain engineering, which can be efficiently applied during fabrication processes, has become a compulsory technique to give an enhanced performance in MOSFET devices [1]. Recent theoretical studies on strain have shown that the uniaxial strain plays a significant role on the transport properties in nanowire FETs [2]–[6].

The bulk crystal symmetry is not preserved in nanowire structure so the quantitative results obtained from the bulk *k.p* parameters give rise to inappropriate description in the ultra-narrow devices. For this reason, continually using the bulk *k.p* parameters in the non-atomistic *k.p* method is expected to bring errors when the nanowire diameter becomes smaller. Though an empirical tight-binding (TB) approach would be more rigorous for the quantum calculations, it takes enormous computational burden so only ultra-narrow nanowires have been treated [7], [8].

Hence, a promising solution is to use the *k.p* method with modified parameters by benchmarking with the atomistic model such as TB, which will give sufficiently accurate results comparable to atomistic calculations in a-few-nanometer devices with significantly reduced computational time.

In this paper, band structures of the SiNWs by the *k.p* method using the bulk parameters and tuned parameters are compared and their behaviors of valence band edge (VBE), hole effective mass (m^*), and the energy difference between top two valence bands (ΔE_V) against applied strain are examined. The characteristics of the on-current (I_{on}) in unstrained/strained-SiNWs are described as a function of channel length (L) over channel width (W). Especially, we calculate the on-current increase rate of I_{on} in the strained-SiNWs (I_{on}^{st}) over I_{on} in the unstrained-SiNWs (I_{on}^{unst}) and investigate its dependence on L/W.

II. Methodology

To describe the hole transport in the valence band, we use an in-house tool based on the 6-band *k.p* method with the *k.p* parameters adjusted against the sp^3s^* TB model [9]. The simulated devices are three-dimensional (3D) rectangular silicon nanowire FETs (SiNWs) with gate-all-around (GAA) structure as shown in Fig. 1. The source and drain regions of MOSFETs are heavily p-doped ($\sim 10^{20} cm^{-3}$) whereas the channel is intrinsic. The SiO_2 oxide thickness is assumed to be 1 nm and the drain bias V_{DS} is 0.5 V. The parameter L/W is varied

978-1-4799-5288-5/14/$31.00

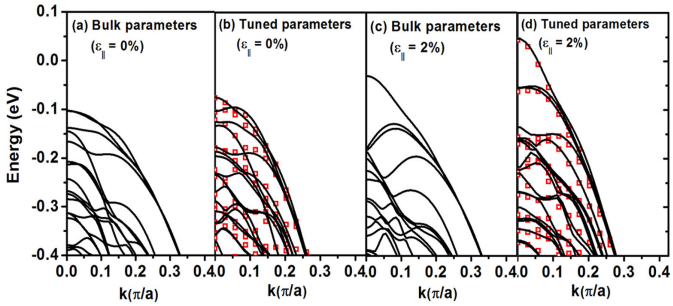

Fig. 2: Unstrained band structures of [100]-SiNW with W = 5 cross section by (a) *k.p* method using the bulk parameters, (b) the *k.p* method using the tuned parameters (solid lines) and TB (open square symbols) approach. The band structures under $\varepsilon_{||}$ = 2% compressive strain by (c) *k.p* method using the bulk parameters, (d) *k.p* method using the tuned parameters (solid lines) and TB (open squares symbols) approach.

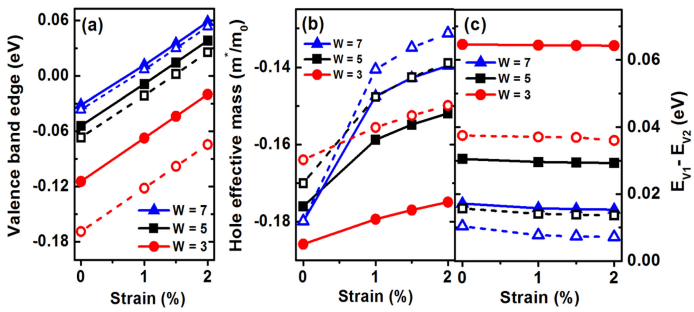

Fig. 3: Variation of the (a) valence band edge (b) hole effective masses, and (c) energy difference between top two valence bands of [110]-SiNWs as a function of strain for different wire widths (W) by using the bulk *k.p* parameters (dashed lines) and tuned *k.p* parameters (solid lines).

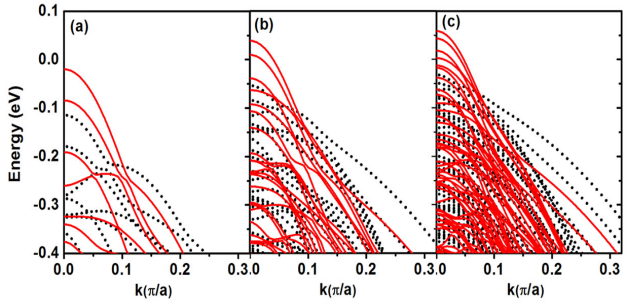

Fig. 4: Valence band structure of unstrained (black short dots) and uniaxial strained (red solid lines) [110]-SiNWs of (a) W = 3 (b) W = 5 (c) W = 7 nm wire width with the uniaxial compressive strain ($\varepsilon_{||}$ = 2%) by using the tuned *k.p* method.

from 2 to 7 where L and W are individually changed.

The compressive uniaxial stress $\varepsilon_{||} = 0 \sim 2\%$ is applied along the transport direction of Si channel. The approach to realize the strain effects with the multi-band *k.p* descriptions is detailed in [10]. We use a full quantum treatment by employing the non-equilibrium Green's function approach and self-consistently solving Schrodinger-Poisson equations in the coupled mode space. All the physical quantities expressed with upper subscript of '*unst*' are for unstrained-SiNWs and '*st*' are for strained-SiNWs.

III. Results

A. *k.p parameters in Band structure*

The band structures calculated by using the bulk and tuned *k.p* parameters are respectively shown in Fig. 2(a)-(b) under unstrained condition. These results have already been reported in [9] showing that the band structure by using the bulk *k.p* parameters looks quite different from that of TB result while the band structure by using the tuned *k.p* parameters is much closer to the TB calculation. We have found that using the tuned *k.p* parameters under strain condition is still valid for the *k.p* band calculation which gives the similar results to the TB band as shown in Fig. 2(c)-(d). These tuned *k.p* parameters can be applied to other directions (*i.e.*, [110] or [111]), although only [100] band structures are shown here.

In Fig. 3(a)-(c), the valence band edge (VBE), numerically calculated hole effective masses (m^*), and the energy difference between top two valence bands (ΔE_V, as in $E_{V1} - E_{V2}$) of [110]-SiNWs by using the tuned *k.p* parameters and the bulk *k.p* parameters for different W's are compared. For all W's, the VBE tends to upshift and the hole effective mass is reduced with compressive strain while the energy difference between the top two valence bands hardly changes (consults Fig. 4). The results obtained from the bulk *k.p* parameters are also displayed in the figure. The main features of the valence bands do not change much when the bulk *k.p* parameters are used so that the overall qualitative trend seems to be similar. However, due to the quantum confinement effects, the difference between the band structure by using the tuned *k.p* parameter and the band structure by using the bulk *k.p* parameter is increased as the size of nanowire is reduced. Hence, using the tuned *k.p* parameters is important in the quantum simulation as the nanowire size decreases.

B. *On-current (I_{on}) Calculation*

Fig. 5(a),(b) show I_{on}^{unst} and I_{on}^{st} of [110]-SiNWs as a function of L/W, respectively. The off-current (I_{off}) criteria is set to $100nA/\mu m$ and I_{on} is normalized by W. For unstrained-devices, I_{on}^{unst} is increased as W becomes smaller and L becomes longer. I_{on}^{st}, however, shows weak dependency on W: that is, large sized [110]-SiNWs can have comparable performance to that of smaller sized

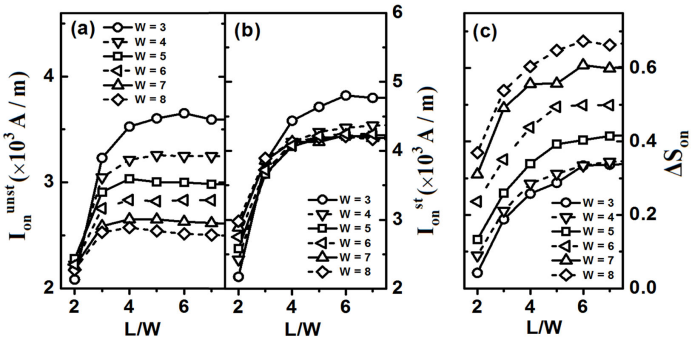

Fig. 5: I_{on} of [110] (a) unstrained-SiNWs, (b) strained-SiNWs, and (c) ΔS^{on} as a function of L/W.

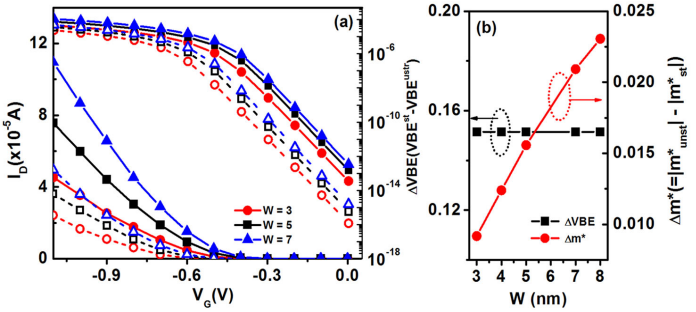

Fig. 6: (a) $I_D - V_G$ characteristics of [110] unstrained (dashed lines) and uniaxial strained (solid lines) SiNWs when L/W = 4. (b) Dependence of ΔVBE (left axis) and m^* (right axis) on W.

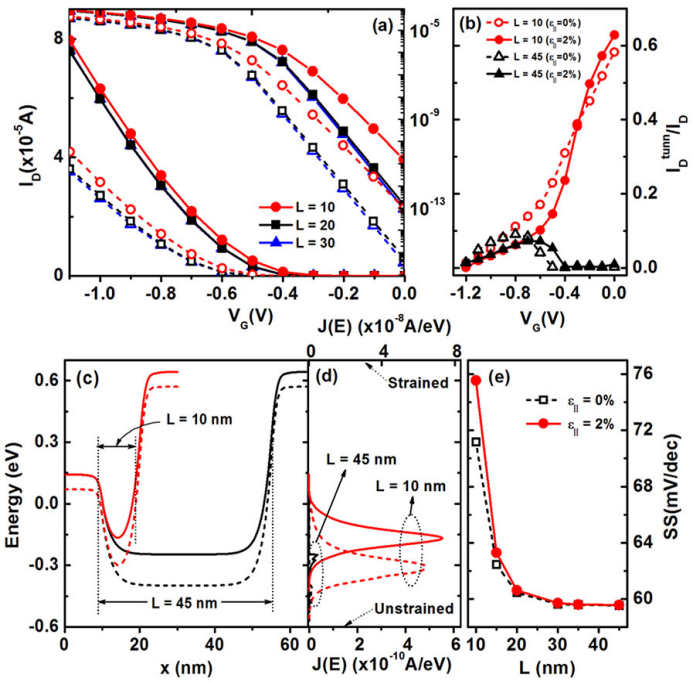

Fig. 7: (a) $I_D - V_G$ characteristics of [110] unstrained (dashed lines) and strained (solid lines) SiNWs for different channel lengths. (b) Contribution of the tunneling current (I_D^{tunn}) to the total current (I_D) as a function of V_G. (c) Example potential profiles in the off-region (V_G = -0.2V) for unstrained (dashed lines) and strained (solid lines) devices and the (d) corresponding current distributions are represented. (e) SS of unstrained (dashed lines) and strained (solid lines) SiNWs with respect to L. W is fixed as 5 nm.

[110]-SiNWs if stress is applied. This result implies that applying uniaxial compressive strain in [110]-SiNWs can be the powerful technique for enhanced hole transport properties instead of reducing the device size into ultra-nano scale.

In Fig. 5(c), the on-current increase rate ($\Delta S^{on} = (I_{on}^{st} - I_{on}^{unst})/I_{on}^{unst}$) as a function of L/W is shown. The first thing to notice is that ΔS^{on} is increased as W becomes larger. As mentioned above, the hole effective mass is reduced by the compressive strain for all W's. We have found that the reduction amount of the effective mass by strain ($\Delta m^* = |m_{unst}^*| - |m_{st}^*|$) is also increased with the increase of W which is clearly shown in Fig. 6(b). Unlike m^*, changes in valence band edge ($\Delta VBE = VBE_{st} - VBE_{unst}$) is almost invariant with respect to W. Consequently, lighter effective mass of wider strained-SiNWs gives rise to significant increase of I_{on} compared to that of in narrow strained-SiNWs under equal stress which can be seen in Fig. 5(b) and Fig. 6(a), respectively.

In terms of the channel length, on the other hand, ΔS^{on} shows decreasing behavior as L becomes shorter even though m^* and VBE have no relevance with the channel length variation. The increase of I_{on}^{st} by strain in the short-channel devices is not as much as that in the long-channel devices. When channel length is decreased, the potential barrier becomes thinner and holes can easily tunnel through the barrier (Fig. 7(c)-(d)). Namely, holes having reduced m^* by strain are able to pass through the barrier more easily than in the case of the unstrained-devices. It gives rises to large tunneling current in the off-region and appears significantly when the channel length is shorter. In Fig. 7(b), we illustrates that the subthreshold current in the relatively short channel case (L = 10 nm) is dominated by the tunneling current while that in the long channel case (L = 45 nm) is almost ignorable. Accordingly, the subtrheshold-swing (SS) value increases with decrease of L as shown in Fig. 7(e) which can be also confirmed in the $I_D - V_G$ characteristics in Fig. 7(a).

IV. Conclusion

In summary, we have examined the hole transport properties in uniaxial strained-SiNWs by using the 6-band *k.p* method. Adequately precise calculation can be performed by using the *k.p* parameters that are tuned against sp^3s^* TB method.

We have investigated the dependence of the on-current increase rate ΔS^{on} on L/W. ΔS^{on} is increased with

the increasing W which implies that the strain impact becomes stronger with larger W. The reduction amount of the effective mass (Δm^*) by strain is proportional to the size of the nanowire so I_{on} of wider SiNWs is remarkably increased by strain. These results demonstrate that even large size of the [110]-SiNWs can have comparable hole transport properties to that of small size of the [110]-SiNWs if compressive stress is applied.

In terms of L, the tunneling probability of holes in the off-region becomes greater in the short-channel devices, and it becomes more noticeable when the hole effective mass is reduced by the strain. The large off-current offsets the increase of I_{on}^{st} in short-channel devices, and therefore ΔS^{on} tends to decrease with shorter L.

ACKNOWLEDGMENT

This research was supported by the Pioneer Research Center Program and the Basic Science Research Program thorough the National Research Foundation of Korea (NRF) Funded by the Ministry of Education, Science and Technology (Grant No. 2012-0000459 and No. 2012-0002120).

REFERENCES

[1] C. Remi, C. Mikael, B. Sylvain, C. David, M. A. Virginie, M. P. Samson, M. Stephane, B. Frederic, G. Gerard, F. Olivier, and P. Thierry, "Strain-Induced Performance Enhancement of Trigate and Omega-Gate Nanowire FETs Scaled Down to 10-nm Width," *IEEE Trans. Electron Devices*, vol. 60, pp. 727-732, Feb. 2013.

[2] V. H. Nguyen, F. Triozon, F. D. R. Bonnet, and Y. M. Niquet, "Performances of strained Nanowire Devices: Ballistic versus Scattering-limited currents," *IEEE Trans. Electron Devices*, vol. 60, pp. 1506-1513, May, 2013.

[3] W. Chern, P. Hashemi, J. T. Teherani, Y. Tao, D. Yuanwei, X. Guangrui, D. A. Antoniadis, J. L. Hoyt, "High mobility high-k-all-around asymmetrically-strained Germanium nanowire trigate p-MOSFETs," *IEEE International Electron Devices Meeting(IEDM)*, pp. 16.5.1-4, Dec. 2012.

[4] F. Conzatti, M. G. Pala, D. Esseni, E. Bano, and L. Selmi, "Strain-Induced Performance Improvements in InAs nanowire Tunnel FETs," *IEEE Trans. Electron Devices*, vol. 59, no. 8, pp. 2085-2092, Aug. 2012.

[5] V. H. Nguyen, "Strain effects on transport properties of Si nanowire devices," *International Conference on Simulation of Semiconductor Processes and Devices (SISPAD)*, pp. 89-92, Sep. 2013.

[6] J. T. Teherani, W. Chern, D. A. Antoniadis, J. L. Hoyt, "Simulation of enhanced hole ballistic velocity in asymmetrically strained-Ge nanowire Trigate pMOSFETs," *IEEE International Electron Devices Meeting(IEDM)*, pp. 32.4.1-4, Dec. 2013.

[7] H. Minari, T. Kitayama, M. Yamamoto, and N. Mori, "Strain Effects on Hole current in silicon nanowire FETs," *International Conference on Simulation of Semiconductor Processes and Devices (SISPAD)*, pp. 207-210, Sep. 2010.

[8] L. Zhang, H. Lou, J. He, and M. Chan, "Uniaxial Strain Effects on Electron Ballistic Transport in Gate-All-Around Silicon Nanowire MOEFETs," *IEEE Trans. Electron Devices*, vol. 58, no. 11, pp. 3829-3836, Nov. 2011.

[9] M. Shin, S. Lee, and G. Klimeck, "Computational Study on the Performance of Si Nanowire pMOSFETs Based on the *k.p* method," *IEEE Trans. Electron Devices*, vol. 57, no. 9, pp. 2274-2283, Sep. 2010.

[10] T. B. Bahder, "Eight-band *k.p* model of strained zinc-blende crystals," *Phys. Rev. B*, vol. 41, no. 17, pp. 11992, Jun. 1990.